Biophys Rep 2025, 11(4):283–290
https://doi.org/10.52601/bpr.2024.240059 https://cstr.cn/32402.14.bpr.2024.240059
Biophysics Reports

RESEARCH ARTICLE

# A single helicase-binding domain of DnaG couples with hexameric helicase DnaB in *Bacillus stearothermophilus*

**Hao Luo[1,2], Wenlin Liu[1,2], Yingqin Zhou[1], Zhongchuan Liu[1], Yuyang Qin[1,2], Ganggang Wang[1] ✉**

[1] Agricultural Microbial Agents Key Laboratory of Sichuan Province, Chengdu Institute of Biology, Chinese Academy of Sciences, Chengdu 610213, China
[2] University of Chinese Academy of Sciences, Beijing 100049, China

Received: 9 November 2024 / Accepted: 18 December 2024

**Abstract** In bacterial DNA replication, helicase DnaB and primase DnaG form the primosome. Helicase DnaB unwinds double-stranded DNA (dsDNA) to provide templates for DNA polymerase, whereas primase DnaG supplies RNA primers to DNA polymerase for the synthesis of Okazaki fragments. How primase DnaG coordinates with helicase DnaB at the DNA replication fork remains unclear. In this study, the interactions between the helicase-binding domain of DnaG (DnaG (HBD)) and DnaB hexamer were studied. A stable ternary complex of $DnaB_6/dT_{16}$/DnaG(HBD) from *Bacillus stearothermophilus* was prepared and the homogeneity of the $DnaB_6/dT_{16}$/DnaG(HBD) complex was verified by dynamic light scattering. The stoichiometry of DnaG(HBD) to process $DnaB_6$ was investigated by isothermal titration calorimetry. The results show that a single primase DnaG binds to $DnaB_6$ in the presence of single-stranded DNA. Based on these results, a model is proposed to explain how the primase DnaG couples with the processing $DnaB_6$ helicase during the Okazaki fragment synthesis cycle. These findings provide valuable insights into the coupling between dsDNA unwinding and RNA primer synthesis in DNA replication.

**Keywords** DNA replication, Primosome, Helicase, Primase, Okazaki fragment

## INTRODUCTION

DNA replication in bacteria is accomplished by the replisome complex, which consists of a dozen proteins. Among them, helicase DnaB and primase DnaG form the primosome (Berger 2008; Enemark and Joshua-Tor 2006; Schlierf *et al.* 2019; Chen *et al.* 2024). DnaB unwinds the double-stranded DNA using energy provided by NTP hydrolysis, and DnaG synthesizes RNA primers for DNA polymerase to synthesize Okazaki fragments (Fernandez and Berger 2021; Kuchta and Stengel 2010). Primase DnaG consists of three domains, an N-terminal regulatory zinc-binding domain (ZBD), a central RNA polymerase domain (RPD), and a C-terminal helicase-binding domain (HBD) (Chintakayala *et al.* 2007; Chintakayala *et al.* 2008; Monachino *et al.* 2020; Rodina and Godson 2006; Syson *et al.* 2005). In *Escherichia coli*, the C-terminal octa-peptide of DnaG could bind to helicase DnaB (Tougu and Marians 1996). In *Bacillus stearothermophilus* (*B. stearothermophilus*), the primase DnaG is attached to the helicase DnaB via direct interaction with the C-terminal helicase-binding domain (HBD) (Chintakayala *et al.* 2007; Chintakayala *et al.* 2008; Syson *et al.* 2005). The interplay between DnaB and DnaG stimulates the activities of both proteins. DnaG increases both the ATPase and the helicase activities of DnaB (Kuchta and Stengel 2010), and DnaB regulates the synthesis of RNA primers by DnaG, including the synthesis efficiency and primer length (Bergsch *et al.* 2019).

The structure of the DnaB hexamer ($DnaB_6$) adopts a

✉ Correspondence: wanggg@cib.ac.cn (G. Wang)

double-layer planar ring with the NTDs in the triangular collar positioned above the ring of CTDs (Bailey *et al.* 2007; Wang *et al.* 2008). In *B. stearothermophilus*, a DnaB hexamer binds three primases, which was observed in the crystal structure of the $DnaB_6$ and primase HBD complex，three primase HBD domains bind to the NTDs of DnaB hexamer (Bailey *et al.* 2007). Corn *et al*. showed that in the presence of an RNA/DNA heteroduplex, the ZBD of one primase may interact with the RPD of a second molecule in trans, which was not detected in the presence of ssDNA (Corn *et al.* 2005). In *B. stearothermophilus*, upon binding to ssDNA, $DnaB_6$ forms a fibrous structure by wrapping around ssDNA to form a right-handed spiral, instead of the planar ring. The rearrangement of subunits in $DnaB_6$ is hypothesized to be essential for the unwinding of dsDNA, the HBD binding sites in $DnaB_6$/ssDNA complex are distinct from that in Apo DnaB hexamer (Itsathitphaisarn *et al.* 2012). Accordingly, how the primase DnaG binds to processing $DnaB_6$ in each cycle of Okazaki fragment synthesis requires further investigations.

In this report, we prepared the $DnaB_6/dT_{16}$/DnaG(HBD) complex and provide direct evidence for the binding ratio of DnaG(HBD) to $DnaB_6$ in the $DnaB_6/dT_{16}$/DnaG(HBD) complex. These results will advance our understanding of primosome priming on the lagging strand of *B. stearothermophilus*.

## RESULTS

### DnaG(HBD) can form a complex with $DnaB_6/dT_{16}$

The crystal structure of $DnaB_6/dT_{16}$ complex was previously reported, here we detected the $DnaB_6/dT_{16}$ binary complex through EMSA experiments (lane 4 in Fig. 1A). The addition of DnaG(HBD) resulted in the formation of a stable ternary complex (Lanes 5–9 in Fig. 1A). The $DnaB_6$/HBD (Fig. 1B) and $DnaB_6/dT_{16}$/HBD (Fig. 1C) complexes were prepared by gel filtration chromatography, the elution volume for $DnaB_6$/HBD is 10.34 mL, and 10.86 mL for $DnaB_6/dT_{16}$/HBD complex. 10 μL samples of the complexes were analyzed by sodium dodecyl sulfate polyacrylamide gel electrophoresis (SDS-PAGE) and Native-PAGE, and the $dT_{16}$ in the protein/nucleic acid complex was detected by SYBR green II staining (Fig. 1C).

The uniformity of the $DnaB_6$/DnaG(HBD) and $DnaB_6/dT_{16}$/DnaG(HBD) complexes was verified by dynamic light scattering (DLS). Typical hydrodynamic radius distributions of the particles are shown in Fig. 2. Particle sizes were obtained from cumulant analysis of the measured DLS correlation functions and thus represent an average over the whole size distribution. Average hydrodynamic radii (from cumulant analysis) of $DnaB_6$/DnaG(HBD) and $DnaB_6/dT_{16}$/DnaG(HBD) were determined to be 6.9 ± 0.1 nm and 6.7 ± 0.1 nm, respectively (Fig. 2).

### The proportion of helicase to primase in $DnaB_6/dT_{16}$/HBD complex

$DnaB_6$ has been proposed to adopt continuous subunit rearrangements during translocation (Itsathitphaisarn *et al.* 2012). This raises the question as to how primase DnaG coordinates with the dynamic $DnaB_6$ for priming because DnaG binding sites may be formed and used sequentially. To resolve this question, Isothermal titration calorimetry (ITC) was used to study the thermodynamic aspects of the binding between DnaG(HBD) and the $DnaB_6/dT_{16}$ complex. The $DnaB_6/dT_{16}$ complex was prepared by gel filtration chromatography. The binary complex was analyzed by SDS-PAGE gel and the $dT_{16}$ in the protein/nucleic acid complex was detected by SYBR green II staining (Fig. 3A). The homogeneity of the $DnaB_6/dT_{16}$ complex was verified by DLS (Fig. 2C). The ITC measurements were performed to evaluate the binding ratio of DnaG(HBD) to $DnaB_6/dT_{16}$ complex. The binding isotherm and plotted titration curve for the binding of DnaG(HBD) to $DnaB_6/dT_{16}$ is shown in Fig. 3B. The data fit best to a single binding site model, yielding a binding stoichiometry of one DnaG(HBD) per $DnaB_6/dT_{16}$ complex. Similar results were obtained in the reverse titration (Fig. 3C). At the same time, the DnaB hexamer was titrated by DnaG(HBD), and the data results in the binding ratio of three DnaG(HBD) per DnaB hexamer in the absence of ssDNA. The stoichiometry($n$), equilibrium dissociation constant ($K_d$) and the thermodynamic parameters obtained from at least three independent ITC experiments are summarized in Table 1.

In bacteriophage T7, the primase is linked covalently to the helicase as a bifunctional protein. Thus, six primase domains stack onto the helicase ring at the DNA replication fork (Gao *et al.* 2019; Kulczyk *et al.* 2017). In *B. stearothermophilus*, three DnaG (HBD) molecules bind to the NTD trimer interface of the $DnaB_6$ ring (Bailey *et al.* 2007). When DnaB binds to ssDNA, a helical filament shape instead of a ring was observed (Itsathitphaisarn *et al.* 2012), and the conformational change led to the disruption of the DnaG (HBD) binding sites. Accordingly, less of DnaG (HBD) binds to the $DnaB/dT_{16}$ complex.

 

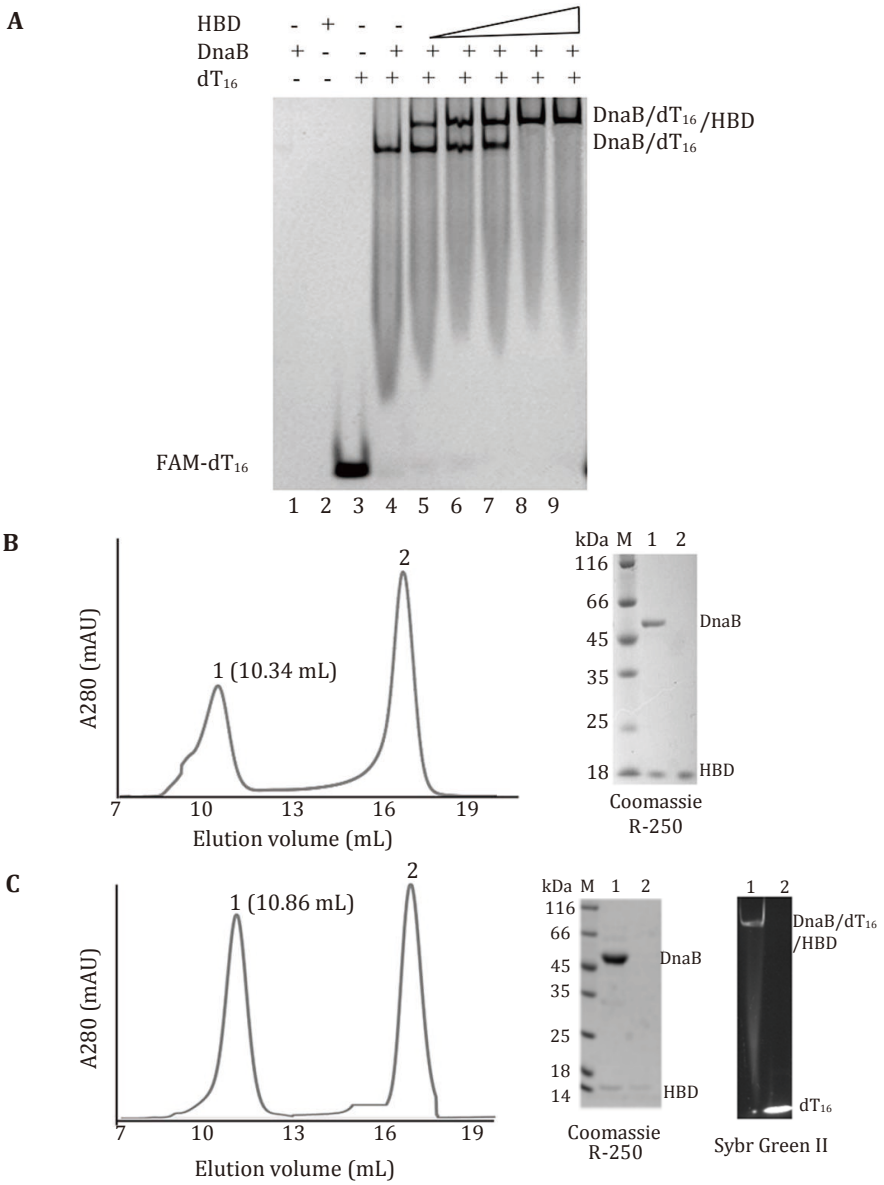


**Fig. 1** DnaG(HBD) and $DnaB_6/dT_{16}$ form a ternary complex. **A** EMSA experiment. Lane 1, DnaG(HBD) (10 pmol); Lane 2, DnaB (8 pmol); Lane 3, $dT_{16}$ (10 pmol, 5'-6-FAM); Lanes 4–9, 8 pmol DnaB and 10 pmol $dT_{16}$ were used in the binding assays and DnaG(HBD) was added at 0, 1, 3, 5, 10 and 15 pmol, respectively. Samples were analyzed using 8% native PAGE. **B** The $DnaB_6$/DnaG(HBD) complex was separated by gel filtration and analyzed by SDS-PAGE. **C** The $DnaB_6/dT_{16}$/DnaG(HBD) complex was separated by gel filtration and analyzed by SDS-PAGE and native PAGE. The SDS-PAGE gel was stained with Coomassie R-250 and the native PAGE was stained with SYBR green. The result shows that both proteins and DNA were eluted in a single peak

## DISCUSSION

In this report, ITC analysis was used to show that one primase interacts with the helicase in the presence of ssDNA. We believe that this is the first time the stoichiometry of primase DnaG to $DnaB_6$ in the $DnaB_6/dT_{16}$/DnaG(HBD) complex has been validated experimentally. In eukaryotic DNA replication, one primase was also observed to associate with the DNA polymerase for lagging strand synthesis (Sun *et al.* 2015). In *E. coli*, priming is initiated once per 1–3 kb of genomic DNA. DnaG is recruited to the replication fork via HBD binding to $DnaB_6$, which recognizes a specific initiation site to produce an RNA primer (Bergsch *et al.* 2019; Chen *et al.* 2024; Jameson and Wilkinson 2017; Wu *et al.* 1992). After priming, the primase subsequently interacts with the clamp loader for the primer handoff to DNA polymerase and then leaves the fork (Chang

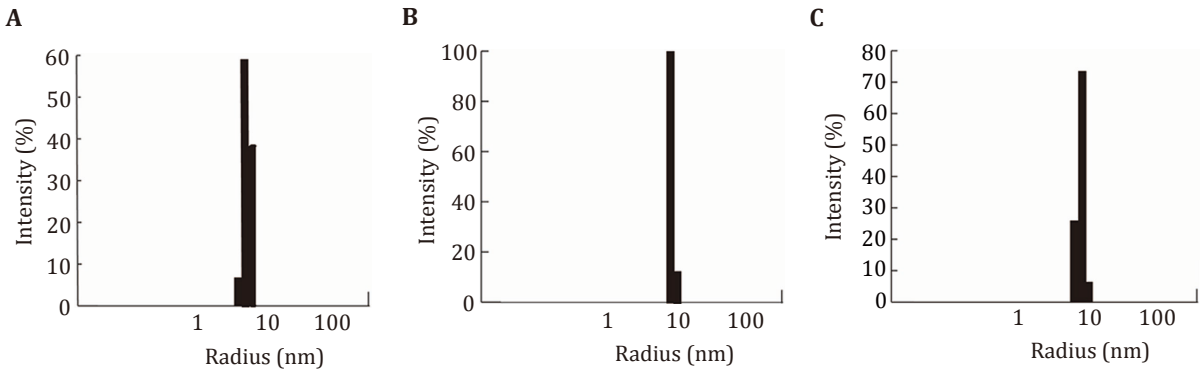


**Fig. 2** Detection of the uniformity of the complexes by dynamic light scattering. **A** $DnaB_6$/DnaG(HBD). **B** $DnaB_6/dT_{16}$/DnaG(HBD). **C** $DnaB_6/dT_{16}$. The mean radii of $DnaB_6$/DnaG(HBD), $DnaB_6/dT_{16}$/DnaG(HBD) and $DnaB_6/dT_{16}$ at 2 mg/mL are 6.9 ± 0.1 nm, 6.7 ± 0.1 nm and 6.6 ± 0.1 nm, respectively

and Marians 2000; Tougu *et al.* 1994; Wu *et al.* 1992). Therefore, the 1:1 stoichiometry of DnaG(HBD) to $DnaB_6$ coordinates the distributive action of DnaG with the structural rearrangement of processing $DnaB_6$ in the cycle of Okazaki fragment synthesis.

By combining our data with the previous biochemical and structural results (Chang and Marians 2000; Itsathitphaisarn *et al.* 2012; Tougu *et al.* 1994; Luo, *et al.* 2019), a model of the primase DnaG at the DNA replication fork in *B. stearothermophilus* can be created. We propose that in the presence of a priming signal one primase DnaG is recruited to the DNA replication fork by HBD binding to the $DnaB_6$ helicase. Subsequently, the ZBD/RPD recognizes a specific initiation site and moves away for priming and the RNA primer is passed to the DNA polymerase (Lee *et al.* 2012). After priming, the HBD binding site on $DnaB_6$ undergoes a conformational change that causes primase DnaG to disassociate from $DnaB_6$ (Itsathitphaisarn *et al.* 2012) (Fig. 4). In this mode of primosome organization, the distance between HBD and the ZBD/RPD may increase during primer elongation. The 30-residue linker between HBD and ZBD/RPD should facilitate structural reorganization of the ZBD/RPD to accomplish primer synthesis (Luo *et al.* 2019). Although this model is based on data from *B. stearothermophilus*, it may be a representative of other pathogen bacteria, such as *E. coli* and *Staphylococcus aureus*, since the counterparts of helicase DnaB and primase DnaG are conserved in these bacteria (Chang and Marians 2000; Kuchta and Stengel 2010; Patel *et al.* 2011; Wang *et al.* 2008). Conversely, bacterial helicase DnaB and primase DnaG are quite distinct from their counterparts found in humans (Baranovskiy *et al.* 2015; Baranovskiy *et al.* 2016). Thus, the primosome represents an ideal target for the development of novel antibiotics (Ilic *et al.* 2018). The data reported here should facilitate the design of new classes of antibiotics that target the DnaG binding site.

In conclusion, the results presented define the architecture of the primosome in *B. stearothermophilus* and provide insights into how the helicase and primase in DNA replication are physically and functionally coupled. This work also paved the curb for exploring the helicase and primase interplay *in vivo*. To better define the chemical basis for helicase and primase coupling, further investigations are required to determine the three-dimensional structure of $DnaB_6$/ssDNA/DnaG ternary complexes.

## MATERIALS AND METHODS

### Protein expression and purification

The DnaB and DnaG(HBD) proteins were prepared as described in the previous publications (Pan *et al.* 1999; Yang and Wang 2016; Zhou *et al.* 2017). Briefly, the PCR amplified genes dnaB, and dnaG (hbd) from *B. stearothermophilus* were inserted into the pGEX-6p-1 vector. The primers of DnaB-F (5′-CGCGGATCCTATGAGCGAGCTGTTTTCAGAA-3′), HBD-F (5′-CGCGGATCCAAGTTGCTGCCGGCTTTTCA-3′) with BamHI site and DnaB-R (5′-CCGCGCCTCGAGTTACGCCCCCGGCGGAATTTG-3′), HBD-R (5′-CCGCGCCTCGAGTTATGAGGAAGATAACATTT-3′) with XhoI site were made (Sangon Biotech Co., Ltd). All constructs were confirmed by DNA sequencing. The positive constructs were transformed into *E. coli* BL21 (DE3) cells for expression of the recombinant proteins. The cells were grown to an $OD_{600}$ of 0.4–0.6 in LB medium containing 100 μg/mL ampicillin at 37°C. Overexpression of these proteins was induced by the addition

 

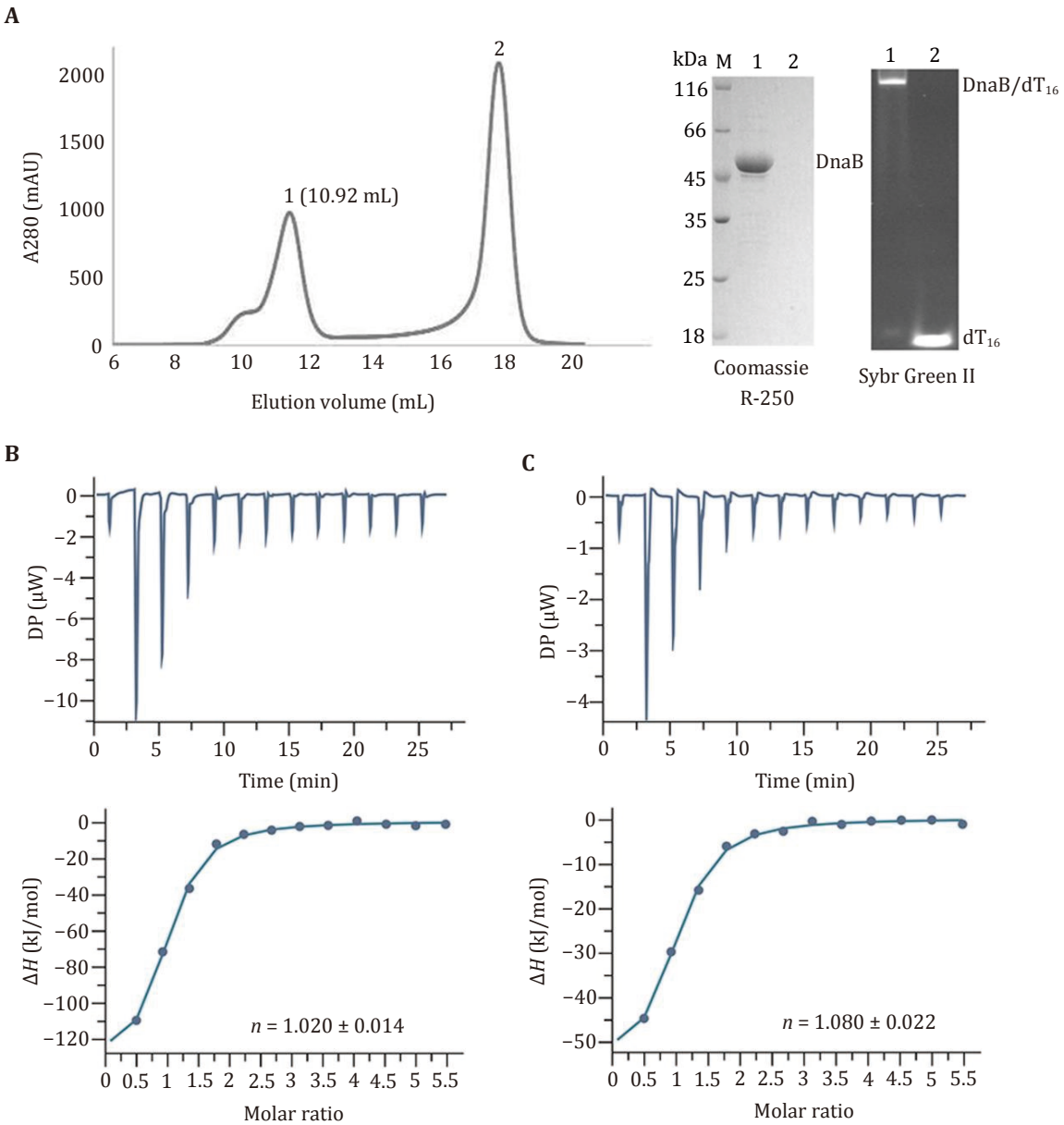


**Fig. 3** ITC measurements of the interactions between DnaG(HBD) and $DnaB_6/dT_{16}$ complex. **A** Preparation and detection of the $DnaB_6/dT_{16}$ complex. The $DnaB_6/dT_{16}$ complex was separated by gel filtration and analyzed by SDS-PAGE. The gel was stained initially with Coomassie R-250 and then with SYBR green. The results show that the $DnaB_6/dT_{16}$ binary complex was prepared successfully. **B** The upper panel represents a typical raw trace of the titration of DnaG(HBD) to the $DnaB_6/dT_{16}$ complex at 25°C. The lower panel shows the result of an integration of heat exchange for each injection fitted with the one-set-of-sites model using the MicroCal PEAQ-ITC analysis software supplied by the manufacturer. **C** Reverse titration of the $DnaB_6/dT_{16}$ complex to DnaG(HBD). The upper panel represents a typical calorimetric titration and the lower panel shows the resulting integrated binding isotherm at 25°C

of IPTG to a final concentration of 0.2 mmol/L, and cells were grown for a further 16 h at 16°C. For purification of recombinant proteins, *E. coli* cells were harvested by centrifugation, and the cells were resuspended in Buffer A (25 mmol/L Tris-HCl, pH 8.0, 300 mmol/L NaCl, 1 mmol/L DTT) and lysed by sonication. After clarification by centrifugation, the GST-fusion proteins were isolated by Sepharose 4B affinity chromatography, and the GST tag was removed by digestion with PreScission protease at 4°C overnight. Proteins were then purified using source 15Q (GE, USA) ion-exchange chromatography followed by passage through a Superdex-200/Superdex-75 gel-filtration column. The proteins were concentrated to ~10 mg/mL in Buffer B

**Table 1** Thermodynamic parameters for the interaction between $DnaB_6/dT_{16}$ and DnaG(HBD)

| Complexes | *n* | $K_d$ (μmol/L) | Δ*H* (kJ/mol) | Δ*G* (kJ/mol) | TΔ*S* (kJ/mol) |
|---|---|---|---|---|---|
| HBD-$DnaB_6/dT_{16}$(1) | 1.020 ± 0.014 | 1.13 ± 0.22 | −94.9 ± 2.21 | −35.5 | 64.5 |
| HBD-$DnaB_6/dT_{16}$(2) | 0.981 ± 0.026 | 1.07 ± 0.13 | −93.0 ± 4.39 | −34.7 | 58.3 |
| HBD-$DnaB_6/dT_{16}$(3) | 1.090 ± 0.073 | 0.96 ± 0.26 | −95.3 ± 6.9 | −30.6 | 64.7 |
| $DnaB_6/dT_{16}$-HBD(1) | 0.987 ± 0.049 | 1.01 ± 0.33 | −46.7 ± 3.99 | −33.4 | 13.3 |
| $DnaB_6/dT_{16}$-HBD(2) | 1.080 ± 0.022 | 1.11 ± 0.24 | −38.4 ± 1.28 | −35.0 | 3.37 |
| $DnaB_6/dT_{16}$-HBD(3) | 1.050 ± 0.022 | 0.89 ± 0.16 | −40.8 ± 5.32 | −31.5 | 9.3 |

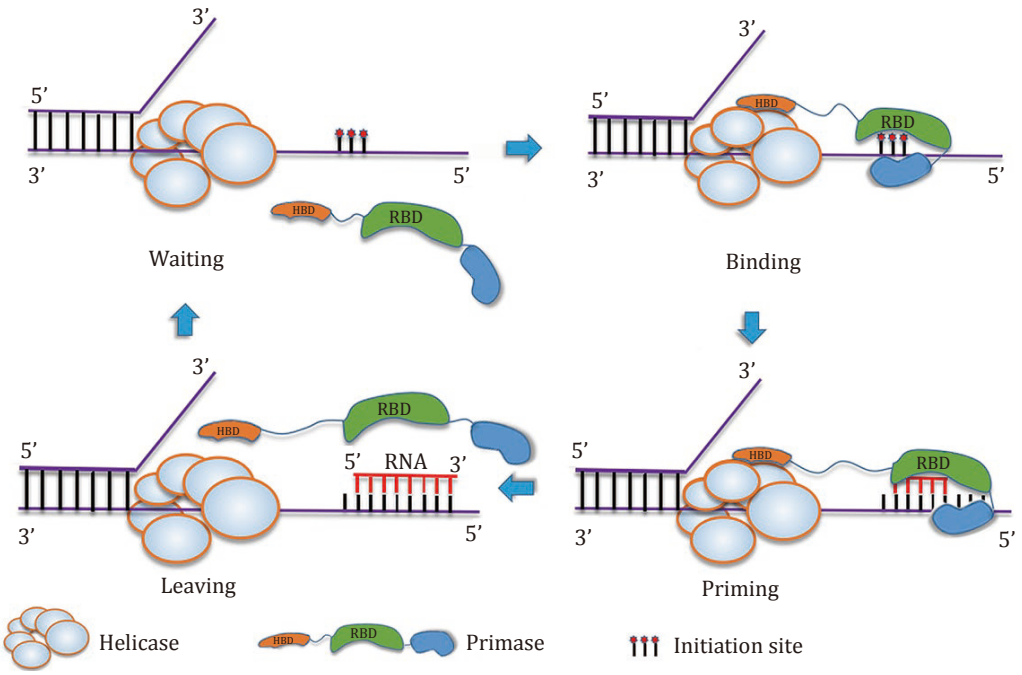


**Fig. 4** A model of the primosome priming on the lagging strand in *B. stearothermophilus*

(25 mmol/L Tris-HCl, pH 8.0, 100 mmol/L NaCl, 1 mmol/L DTT) for further experiments.

### Electrophoretic mobility gel shift assay (EMSA)

The formation of $DnaB/dT_{16}$/DnaG(HBD) complex was resolved by EMSA experiments. The 8 pmol DnaB was mixed with 25% molar excess $dT_{16}$ and kept at 4°C for 30 min, and then the DnaG(HBD) was added for incubation at 4°C for 20 min, the DnaG(HBD) was added at 1, 3, 5, 10 and 15 pmol, respectively. The binding buffer contained 25 mmol/L Tris pH 8.0, 100 mmol/L NaCl, 10% glycerol, 1 mmol/L DTT, 5 mmol/L $MgCl_2$ and 2 mmol/L ATP, the total reaction volume was 20 μL. The samples were analyzed using 6% Native-PAGE. The gel was photographed using a Geldoc XR+ system (Bio-rad, Hercules, CA). The DNAs used in EMSA were single-stranded DNA labeled at the 5'-end with 6-carboxyfluorescein (6-FAM) (Sangon Biotech Co., Ltd).

### Preparation of the complexes

30 μmol/L $DnaB_6$ (100 μL) in Buffer C (25 mmol/L Tris-HCl, pH 8.0, 100 mmol/L NaCl, 1 mmol/L DTT, 5 mmol/L $MgCl_2$) was incubated with 5-fold molar excess of HBD (25 μL) for 30 min at 4°C to form the complex. The complex of $DnaB_6/dT_{16}$ was prepared by incubating 30 μmol/L of $DnaB_6$ (100 μL) in Buffer C with 1 mmol/L ATPγS and 3-fold molar excess of ssDNA for 30 min at 4°C. As to the complex of $DnaB_6/dT_{16}$/DnaG(HBD), 30 μmol/L of $DnaB_6$ (100 μL) in Buffer C

 

was incubated with 1 mmol/L ATPγS and 3-fold molar excess of ssDNA for 30 min at 4°C. Subsequently, 5-fold molar excess of HBD (25 μL) was added and this solution was incubated for 30 min at 4°C. Samples were replenished to 150 μL with Buffer C and purified by Superdex™ 200 10/300 GL size exclusion chromatography (GE, USA) (Bailey *et al.* 2007; Itsathitphaisarn *et al.* 2012). The concentration of the complex samples was determined by a Nanodrop lite UV-Vis spectrophotometer (Thermol, USA) (Chen *et al.* 2021). 10 μL samples of complexes purified by Superdex™ 200 10/300 GL were detected by denaturing and non-denaturing gel electrophoresis, and the nucleic acids in the complexes, as well as displaced nucleic acids were colored by SYBR green II. And then the 500 μL samples in the middle of the peaks were concentrated for ITC analysis.

### Dynamic light scattering (DLS) measurements

The size of the samples was determined by DLS measurements in a 50-μL low volume quartz cuvette using a Dynapro Nanostar (Wyatt, Beijing, China) at 25°C. The distribution represents the average of five measurements, and each measurement consisted of ten 0.5-s acquisitions. The time-dependent correlation function $G(\tau)$ was measured for different samples in Buffer C. $D_t$ is related to the hydrodynamic radius $R_h$ of particles through the Stokes-Einstein relation $D_0 = k_B T/6\pi\eta R_h$, where $k_B$ is Boltzmann's constant ($1.381 \times 10^{-23}$ J/K), $T$ is the absolute temperature and $\eta$ is the absolute (or dynamic) viscosity of the solvent (Bordi *et al.* 2001; Chiasserini *et al.* 2015; Dahani *et al.* 2015). The measured autocorrelation functions were analyzed using the cumulants method to evaluate the uniformity and average sizes of the particles (Frisken 2001).

### Isothermal titration calorimetry (ITC) measurements

ITC was employed to measure the stoichiometric ratio and binding affinities of two components. All samples were prepared in a buffer containing 25 mmol/L Tris, pH 8.0, 100 mmol/L NaCl. The samples were centrifuged to remove any precipitate before the experiments. All measurements were carried out at 25°C by using a PEAQ-ITC instrument (Malvern, UK). The sample concentrations in the titration needle and sample cell were 200 μmol/L and 10 μmol/L, respectively. Each set of titration experiments was repeated three times. The binding curves were analyzed, and dissociation constants ($K_d$) were determined by a "one-set-of-sites" model using the MicroCal PEAQ-ITC analysis software supplied by the manufacturer (Malvern, UK).

**Acknowledgements** This work was supported by the project from the Science and Technology Department of Sichuan Province (2022YFSY0028), the grants from the National Natural Science Foundation of China, NSFC (31470742, U1432102, 31700664, 31270783) and the 100 Talents Program of the Chinese Academy of Sciences.

**Compliance with Ethical Standards**

**Conflict of interest** Hao Luo, Wenlin Liu, Yingqin Zhou, Zhongchuan Liu, Yuyang Qin and Ganggang Wang declare that they have no conflict of interests.

**Human and animal rights and informed consent** This article does not contain any studies with human and animal subjects performed by any of the authors.



## References

Bailey S, Eliason WK, Steitz TA (2007) Structure of hexameric DnaB helicase and its complex with a domain of DnaG primase. Science 318(5849): 459–463

Baranovskiy AG, Zhang Y, Suwa Y, Babayeva ND, Gu J, Pavlov YI, Tahirov TH (2015) Crystal structure of the human primase. J Biol Chem 290(9): 5635–5646

Baranovskiy AG, Zhang Y, Suwa Y, Gu J, Babayeva ND, Pavlov YI, Tahirov TH (2016) Insight into the human DNA primase interaction with template-primer. J Biol Chem 291(9): 4793–4802

Berger JM (2008) SnapShot: nucleic acid helicases and translocases. Cell 134(5): 888–888

Bergsch J, Allain FH, Lipps G (2019) Recent advances in understanding bacterial and archaeoeukaryotic primases. Curr Opin Struct Biol 59: 159–167

Bordi F, Cametti C, De Luca F, Carlini E, Palmerini CA, Arienti G (2001) Hydrodynamic radii and lipid transfer in prostasome self-fusion. Arch Biochem Biophys 396(1): 10–15

Chang P, Marians KJ (2000) Identification of a region of *Escherichia coli* DnaB required for functional interaction with DnaG at the replication fork. J Biol Chem 275(34): 26187–26195

Chen J, Luo H, Tao M, Liu Z, Wang G (2021) Quantitation of nucleoprotein complexes by UV absorbance and Bradford assay. Biophys Rep 7(6): 429–436

Chen J, Luo H, Zhang Z, Xu S, Wang G (2024) Studies on the interaction between DnaG primase and ssDNA template in *Mycobacterium tuberculosis*. Prog. Biochem. Biophys 51(8): 1920–1934

Chiasserini D, Mazzoni M, Bordi F, Sennato S, Susta F, Orvietani PL, Binaglia L, Palmerini CA (2015) Identification and partial characterization of two oppulations of prostasomes by a combination of dynamic light scattering and Pproteomic analysis. J Membr Biol 248(6): 991–1004

Chintakayala K, Larson MA, Grainger WH, Scott DJ, Griep MA, Hinrichs SH, Soultanas P (2007) Domain swapping reveals that the C- and N-terminal domains of DnaG and DnaB, respectively, are functional homologues. Mol Microbiol 63(6): 1629–1639

Chintakayala K, Larson MA, Griep MA, Hinrichs SH, Soultanas P (2008) Conserved residues of the C-terminal p16 domain of primase are involved in modulating the activity of the bacterial primosome. Mol Microbiol 68(2): 360–371

Corn JE, Pease PJ, Hura GL, Berger JM (2005) Crosstalk between primase subunits can act to regulate primer synthesis in trans. Mol Cell, 20(3): 391–401

Dahani M, Barret LA, Raynal S, Jungas C, Pernot P, Polidori A, Bonneté F (2015) Use of dynamic light scattering and small-angle X-ray scattering to characterize new surfactants in solution conditions for membrane-protein crystallization. Acta Crystallogr F Struct Biol Commun, 71(Pt 7): 838–846

Enemark EJ, Joshua-Tor L (2006) Mechanism of DNA translocation in a replicative hexameric helicase. Nature, 442(7100): 270–275

Fernandez AJ, Berger JM (2021) Mechanisms of hexameric helicases. Crit Rev Biochem Mol Biol, 56(6): 621–639

Frisken BJ (2001) Revisiting the method of cumulants for the analysis of dynamic light-scattering data. Applied Optics, 40(24): 4087–4091

Gao Y, Cui Y, Fox T, Lin S, Wang H, de Val N, Zhou ZH, Yang W (2019) Structures and operating principles of the replisome. Science 363(6429): eaav7003. https://doi.org/10.1126/science.aav7003

Ilic S, Cohen S, Singh M, Tam B, Dayan A, Akabayov B (2018) DnaG primase-A target for the development of novel antibacterial agents. Antibiotics (Basel), 7(3): 72. https://doi.org/10.3390/antibiotics7030072

Itsathitphaisarn O, Wing RA, Eliason WK, Wang J, Steitz TA (2012) The hexameric helicase DnaB adopts a nonplanar conformation during translocation. Cell, 151(2): 267–277

Jameson KH, Wilkinson AJ (2017) Control of initiation of DNA replication in *Bacillus subtilis* and *Escherichia coli*. Genes (Basel), 8(1): 22. https://doi.org/10.3390/genes8010022

Kuchta RD, Stengel G (2010) Mechanism and evolution of DNA primases. Biochim Biophys Acta 1804(5): 1180–1189

Kulczyk AW, Moeller A, Meyer P, Sliz P, Richardson CC (2017) Cryo-EM structure of the replisome reveals multiple interactions coordinating DNA synthesis. Proc Natl Acad Sci USA 114(10): E1848–E1856

Lee SJ, Zhu B, Akabayov B, Richardson CC (2012). Zinc-binding domain of the bacteriophage T7 DNA primase modulates binding to the DNA template. J Biol Chem 287(46): 39030–39040 .

Luo H, Liu WL, Zhou YQ, Tao M, Liu ZC, Wang GG (2019). The study on the solution structure of full length primase from *Bacillus subtilis*. Prog. Biochem. Biophys 46: 1101–1109

Monachino E, Jergic S, Lewis JS, Xu ZQ, Lo ATY, O'Shea VL, Berger JM, Dixon NE, van Oijen AM (2020) A primase-induced conformational switch controls the stability of the bacterial replisome. Mol Cell 79(1): 140–154

Pan H, Bird LE, Wigley DB (1999) Cloning, expression, and purification of *Bacillus stearothermophilus* DNA primase and crystallization of the zinc-binding domain. Biochim Biophys Acta 1444(3): 429–433

Patel SS, Pandey M, Nandakumar D (2011) Dynamic coupling between the motors of DNA replication: hexameric helicase, DNA polymerase, and primase. Curr Opin Chem Biol, 15(5): 595–605

Rodina A, Godson GN (2006) Role of conserved amino acids in the catalytic activity of *Escherichia coli* primase. J Bacteriol 188(10): 3614–3621

Schlierf M, Wang GG, Chen XJS, Ha T (2019) Hexameric helicase G40P unwinds DNA in single base pair steps. Elife, 8(17): e42001. https://doi.org/10.7554/eLife.42001

Sun J, Shi Y, Georgescu RE, Yuan Z, Chait BT, Li H, O'Donnell ME (2015) The architecture of a eukaryotic replisome. Nat Struct Mol Biol, 22(12): 976–982

Syson K, Thirlway J, Hounslow AM, Soultanas P, Waltho JP (2005) Solution structure of the helicase-interaction domain of the primase DnaG: a model for helicase activation. Structure 13(4): 609–616

Tougu K, Marians KJ (1996) The extreme C terminus of primase is required for interaction with DnaB at the replication fork. J Biol Chem 271(35): 21391–21397

Tougu K, Peng H, Marians KJ (1994) Identification of a domain of *Escherichia coli* primase required for functional interaction with the DnaB helicase at the replication fork. J Biol Chem 269(6): 4675–4682

Wang G, Klein MG, Tokonzaba E, Zhang Y, Holden LG, Chen XS (2008) The structure of a DnaB-family replicative helicase and its interactions with primase. Nat Struct Mol Biol 15(1): 94–100

Wu CA, Zechner EL, Marians KJ (1992) Coordinated leading- and lagging-strand synthesis at the *Escherichia coli* DNA replication fork. I. Multiple effectors act to modulate Okazaki fragment size. J Biol Chem 267(6): 4030–4044

Yang M, Wang G (2016) ATPase activity measurement of DNA replicative helicase from *Bacillus stearothermophilus* by malachite green method. Anal Biochem 509: 46–49

Zhou Y, Luo H, Liu Z, Yang M, Pang X, Sun F, Wang G (2017) Structural insight into the specific DNA template binding to DnaG primase in bacteria. Sci Rep 7(1): 659. https://doi.org/10.1038/s41598-017-00767-8

 